Lin, Q., Tian, Y., Lu, D., Gong, Q., Du, X. and Gao, Z. (2021) A prediction method of ground volume loss variation with depth induced by tunnel excavation. *Acta Geotechnica*, 16(11), pp. 3689-3707. (doi: 10.1007/s11440-021-01295-6)

A prediction method of ground volume loss variation with depth induced by tunnel excavation

Qingtao Lin[1, a]; Yu Tian[2, a]; Dechun Lu[3, a,*]; Qiuming Gong[4, a]; Xiuli Du[5, a]; Zhiwei Gao[6, b]

([a] Institute of Geotechnical and Underground Engineering, Beijing University of Technology, Beijing 100124, China)

([b] James Watt School of Engineering, University of Glasgow, Glasgow, G12 8LT, UK)

Abstract: A new concept called the transmission ratio of ground volume loss (TRGVL) is proposed to describe the variation law of ground volume loss with depth above the tunnel. Based on the developed Gaussian function, the formula for TRGVL is deduced. Further, the first-order derivative of TRGVL is presented to evaluate the dilation and compression degree of the soil at any depth above the tunnel. A total of 15 cases, involving 8 field project cases and 7 model test cases, are investigated to validate rationality of the proposed formula. The results of field projects and model test cases indicate variation of TRGVL presents four forms. By analysing the volumetric deformation of the soil above the tunnel, formation mechanism of the each form of TRGVL is revealed. Finally, the evolution of the four forms of TRGVL is used to evaluate the disturbance degree of the soil above the tunnel.

Keywords: Tunnel excavation; ground volume loss; surface and subsurface settlement; developed Gaussian function; soil volumetric deformation

[1]Ph.D. Candidate, Institute of Geotechnical and Underground Engineering, Beijing University of Technology, Beijing 100124, China, E-mail: lqt-026@emails.bjut.edu.cn.

[2]Lecturer, Institute of Geotechnical and Underground Engineering, Beijing University of Technology, Beijing 100124, China, E-mail: tianyu@bjut.edu.cn.

[3,*]Professor, Institute of Geotechnical and Underground Engineering, Beijing University of Technology, Beijing 100124, China, E-mail: dechun@bjut.edu.cn. (Corresponding author)

[4]Professor, Institute of Geotechnical and Underground Engineering, Beijing University of Technology, Beijing 100124, China, E-mail: gongqiuming@bjut.edu.cn.

[5]Professor, Institute of Geotechnical and Underground Engineering, Beijing University of Technology, Beijing 100124, China, E-mail: duxiuli@bjut.edu.cn.

[6]Lecturer. James Watt School of Engineering, University of Glasgow, Glasgow, G12 8LT, UK. E-mail: zhiwei.gao@glasgow.ac.uk.

1. Introduction

Tunnel excavation inevitably causes ground disturbance. The soil above the tunnel collapses when the ground is seriously disturbed (Mahmoud et al., 2011; Zhou, 2015; Zheng et al., 2016; Hu et al. 2016). It brings hidden danger to the safety of underground pipelines and surface structures. The ground settlement, as an important index measured in the tunnel project, is usually adopted to reflect the disturbed range of soil (Loganathan and Poulos, 1998; Fang et al., 2012; Lu et al. 2020a). However, for the tunnel engineering with different ground conditions, the disturbance of the soil at depth z is different when the ground settlement at the depth is the same. The ground settlement cannot fully reflect the disturbance state of the soil above the tunnel.

The volumetric deformation reflects the dilation or contraction degree of the soil. More dilation makes the soil looser, so that the disturbance degree induced by tunnelling is larger (Marshall, 2009; Zhou, 2015; Franza, 2017). The volumetric deformation of the soil above the tunnel can be reflected by variation of the ground volume loss with depth (Atkinson and Potts, 1977; Lee et al., 1992; Zhao, 2008; Marshall et al., 2012). The ground volume loss at depth z, $V_l(z)$, decreases with depth when the soil contracts at depth z, but increases with depth when the soil dilates at z. $V_l(z)$ can describe the disturbance degree of the soil above the tunnel. Peck (1969) and Mair et al. (1993) assumed that the ground volume loss at any depth $V_l(z)$ was equal to that at the tunnel excavation section V_l. However, by conducting the centrifuge test in dense sand, Marshall et al. (2012) found that $V_l(z)$ is the maximum at the ground surface and decreases as z increases. On the contrary, $V_l(z)$ is found to increase with z in the test conducted in loose sand by Wang et al. (2016, 2018) and Zhou et al. (2019), with the maximum ground volume loss appearing at the tunnel crown. Unfortunately, a method that can quantitatively describe $V_l(z)$ has not been found.

This work defines transmission ratio of ground volume loss (TRGVL) to describe $V_l(z)$. The formula for TRGVL is developed, and rationality of the proposed formula is validated. Furthermore, the first-order derivative of the proposed formula is presented to reflect the ground deformation feature of the soil above the tunnel. Finally, variation forms of TRGVL and evolution law between different forms are revealed.

2. Transmission ratio of ground volume loss

After a tunnel is excavated, ground volume loss is induced at the excavation section. With the movement and deformation of the soil above the tunnel, the ground volume loss transmits from the tunnel crown to the ground surface. The ground volume loss at depth z, $V_l(z)$, is equal to the difference of $V_l(z_0)$ and volume change (volume increase is positive) of the soil between depth z and z_0, where z_0 is the depth of the tunnel crown. The ratio between $V_l(z)$ and $V_l(z_0)$ can reveal the volume deformation feature of the soil between z and z_0. Therefore, transmission ratio of ground volume loss (TRGVL) is defined as

$$T(z)=\frac{V_l(z)}{V_l(z_0)} \tag{1}$$

$T(z_0)$ is always equal to 1. $T(z) < 1$ when the soil volume increases between z and z_0, and $T(z) > 1$ when the soil volume decreases. $V_l(z)$ is the result of the coupling effect of various factors, including ground condition, geometric factor of the tunnel, and the construction method. $V_l(z_0)$ is mainly affected by geometric factor of the tunnel and the construction method. Hence, the normalized $T(z)$ mainly reflects the effect of ground condition.

In the transverse plane, $V_l(z)$ is equal to the area of the ground settlement trough at z (Peck, 1969; Lee et al., 1999; Wang et al., 2016), as shown in Fig. 1. Based on the formula for ground settlement, we can get

$$V_l(z)=\int_{-\infty}^{+\infty} S(x,z)\ \mathrm{d}x \tag{2}$$

where $S(x, z)$ is the function of the ground settlement trough; x is the horizontal distance from a point to the vertical tunnel centreline.

Substituting Eq. (2) into Eq. (1) yields

$$T(z)=\frac{\int_{-\infty}^{+\infty} S(x,z)\ \mathrm{d}x}{\int_{-\infty}^{+\infty} S(x,z_0)\ \mathrm{d}x} \tag{3}$$

An explicit expression of $T(z)$ can be obtained once $S(x, z)$ is given.

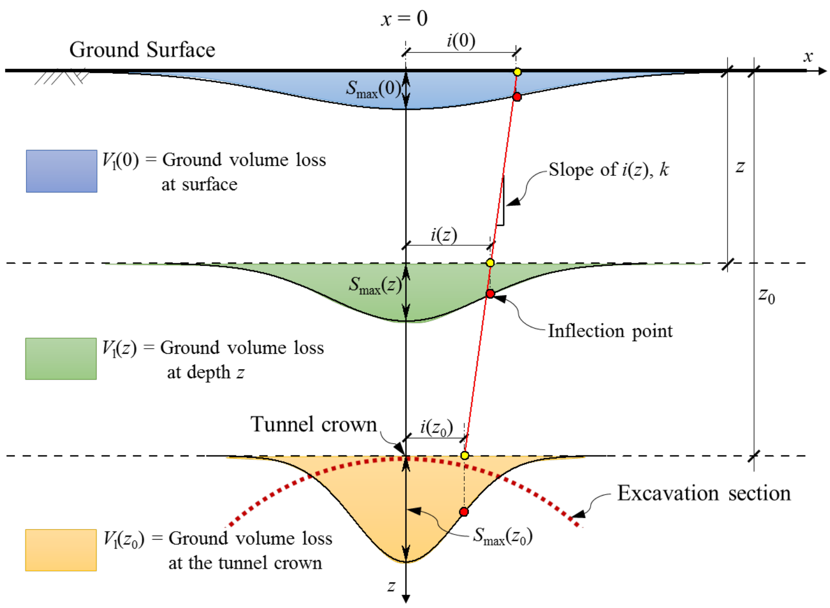

Fig. 1 Schematic diagram of the ground settlement in the transverse plane.

2.1. Ground settlement trough

Many approaches have been proposed to predict the ground settlement trough, such as the empirical methods (Mair et al. 1993; Celestino et al., 2000; Vorster, 2005), analytical methods (Fang et al., 2017; Dong, et al., 2019; Yu et al., 2019; Lu et al., 2019, 2020b; Wang et al., 2020; Zhang et al., 2020), and stochastic medium theory (Yang and Wang, 2011; Zeng and Huang, 2016). Gaussian function is a convenient and reliable empirical method to describe the ground settlement troughs (Mair et al., 1993; Lee, 2009; Marshall et al., 2012, Lu et al., 2020a), and it can be expressed as

$$S(x,z) = S_{\max}(z)\exp\left[\frac{-x^2}{2i(z)^2}\right] \tag{4}$$

where $i(z)$ is the width of the ground settlement trough at z; $S_{max}(z)$ is the maximum settlement at z.

2.1.1 Width coefficient of the settlement trough

Previous research indicates that $i(z)$ is a linear function of z (Boonsiri and Takemura, 2015; Wang et al., 2016). For different ground conditions, $i(z)$ can be formulated by the following

$$i(z) = i(0) - k \cdot z \tag{5}$$

where $i(0)$ is the settlement trough width at the ground surface; k represents the variation rate of the settlement trough width with depth. For clay strata, Mair (1993) suggested that $i(0) = 0.5z_0$, and $k = 0.325$. For sand and gravel stratum, the value of $i(0)$ typically ranges from $0.25z_0$ to $0.45z_0$ (Mair and Taylor, 1997), and the value of k decreases with the increase of V_l (Marshall, 2009).

2.1.2 Maximum ground settlement

Field observations and model test results indicate that $S_{max}(z)$ increases nonlinearly as z increases from 0 to z_0. If $S_{max}(0)$ and $S_{max}(z_0)$ are known, Lu et al. (2020) found that $S_{max}(z)$ can be expressed as

$$S_{\max}(z) = [S_{\max}(0) - S_{\max}(z_0)]\left(1-\frac{z}{z_0}\right)^{\frac{1}{\xi}} + S_{\max}(z_0) \tag{6}$$

where ξ is a parameter reflecting the effects of the ground condition and the tunnel geometric factor. Based on the data from many field projects and model tests (Marshall, 2009; Chen et al., 2011; Mahmoud et al., 2011; Jiang et al., 2013; Zymnis et al., 2013; Pan, 2015; Hu et al., 2016; Wang et al., 2017; Ieronymaki et al., 2018; Lu et al., 2020a), empirical formulas for ξ are determined by fitting the measured $S_{max}(z)$ using Eq. (6) in this work. Values of ξ corresponding to these cases are showed in Fig. 2.

For the clay strata or the complex strata containing the clay layer, ξ decreases approximately linearly as $\ln[S_{max}(0)/S_{max}(z_0)]$ increases (Fig. 2(a)), so that the value of ξ can be estimated by the following

$$\xi = -2.73\ln[(S_{\max}(0)/S_{\max}(z_0)] + 2.33 \tag{7}$$

For the sand or gravel strata, distribution of ξ is approximately linear as $S_{max}(0)/S_{max}(z_0)$ increases, as shown in Fig. 2(b). The distribution of ξ can be described by the following

$$\xi = 0.84(S_{max}(0) / S_{max}(z_0)) + 1.88 \tag{8}$$

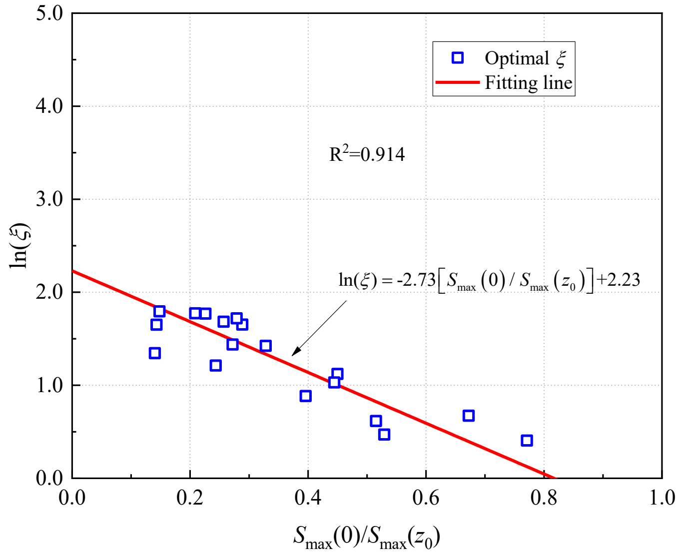

(a) Clay strata or the complex strata containing clay layer

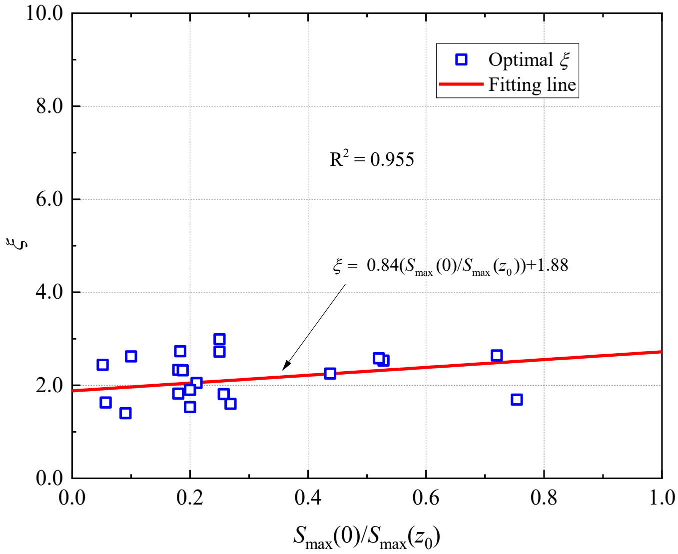

(b) Sand or gravel strata

Fig. 2 Distribution of ξ with $S_{max}(0)/S_{max}(z_0)$.

2.2. Formula for TRGVL

According to the above formulas of $i(z)$ and $S_{max}(z)$, the developed Gaussian function is obtained. Substituting the developed Gaussian function into Eq. (3), one can get

$$T(z) = \left[\left(\frac{S_{max}(0)}{S_{max}(z_0)} - 1 \right) \cdot \left(1 - \frac{z}{z_0} \right)^{\frac{1}{\xi}} + 1 \right] \cdot \frac{i(0) - k \cdot z}{i(0) - k \cdot z_0} \tag{9}$$

In Eq. (9), z_0, $i(0)$, $S_{max}(0)$, and $S_{max}(z_0)$ are known quantities, and k and ξ are parameters. The effect of construction methods on the prediction result of $T(z)$ can be reflected by these parameters and known quantities. $S_{max}(z_0)$ comprehensively reflects the influence of soil volume loss of tunnel excavation section. For the un-shield tunnel, $S_{max}(z_0)$ reflects the support effect of the excavation section. For the shield tunnel, $S_{max}(z_0)$ comprehensively reflects the influence of the support pressure of the cutterhead, over-excavation, and the synchronous grouting, etc. Meanwhile, $i(0)$ and k mainly reflect the effects of the tunnel section shape and the ground condition on $T(z)$.

The first-order partial derivative for $T(z)$ is given as follows

$$T'(z)=\left[\frac{1}{\xi\cdot z_0}\left(1-\frac{S_{max}(0)}{S_{max}(z_0)}\right)\cdot\left(1-\frac{z}{z_0}\right)^{\frac{1-\xi}{\xi}}\right]\cdot\frac{i(0)-k\cdot z}{i(0)-k\cdot z_0}-\left[\left(\frac{S_{max}(0)}{S_{max}(z_0)}-1\right)\cdot\left(1-\frac{z}{z_0}\right)^{\frac{1}{\xi}}+1\right]\cdot\frac{k}{i(0)-k\cdot z_0} \tag{10}$$

The first-order partial derivative of Eq. (9) reflects the volumetric deformation of the soil in the infinitesimal region near depth z. When the soil dilates at z, $V_l(z)$ decreases as z decreases, and $T'(z) > 0$. On the other hand, $V_l(z)$ increases as z decreases when the soil contracts at z, and $T'(z) < 0$.

Eq. (10) has the same parameters with Eq. (9). Based on the test results of Marshall (2009), the effects of k and ξ on variation of $T(z)$ and $T'(z)$ are analyzed, as shown in Fig. 3. In this test condition, the ground volume loss ratio at the excavation section $V_{l,r}$ = 2.5%, z_0 = 0.151 m, $i(0) = 0.62z_0$, $S_{max}(0)$ = 0.34 mm, and $S_{max}(z_0)$ = 0.60 mm.

Fig. 3(a) presents curves of $T(z)$ under different k when $\xi = 2.18$. This figure shows that $T(0)$ becomes larger for a larger k, so that k quantifies the contraction or dilation degree of the soil from the tunnel crown to the ground surface as a whole. Besides, there is a region, in which $T(z) < 1.0$ and the soil shows volumetric dilation as a whole, near the tunnel crown. The smaller the value of k is, the higher this region will be. The negative value of $T'(z)$ indicates the position of the soil dilated above the tunnel. It can be seen from Fig. 3(a), when k becomes larger, the region of the soil dilated expands form a small area near the tunnel crown to entire soil body above the tunnel.

Fig. 3(b) and (c) show curves of $T(z)$ with different ξ when k = 0.10 and 0.40, respectively. It can be seen that ξ has no effect on $T(0)$. In Fig. 3(b), $T(0)$ is smaller than 1, and $T'(z)$ is always larger than 0, indicating that the soil dilates at any depth between the ground surface and the tunnel crown. When ξ is larger than 1, $T'(z)$ decreases as z decreases, and the value of $T'(z)$ is larger for a larger ξ in a limited region above the tunnel crown. It is indicated that the soil near the tunnel crown is much more dilative than that close to the ground surface, and that dilation degree of the soil near the tunnel crown is greater when ξ is relatively large. When ξ is smaller than 1, $T'(z)$ increases as z decreases, indicating the dilation of the soil near the tunnel crown reaches the maximum. In Fig. 3(c), $T(0)$ is larger than 1.0, meaning that the soil above the tunnel crown contracts as a whole. Curves of $T'(z)$ in Fig. 3(c) show that the soil dilates near the tunnel crown but contracts near the ground surface, and the height of the dilative region increases as ξ increases. Therefore, ξ is a parameter reflecting the dilation degree of the soil near the tunnel crown.

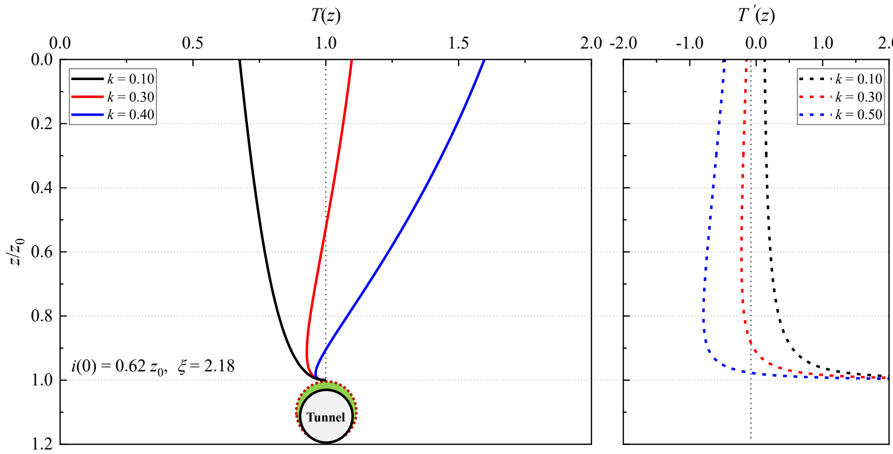

(a) effect of k

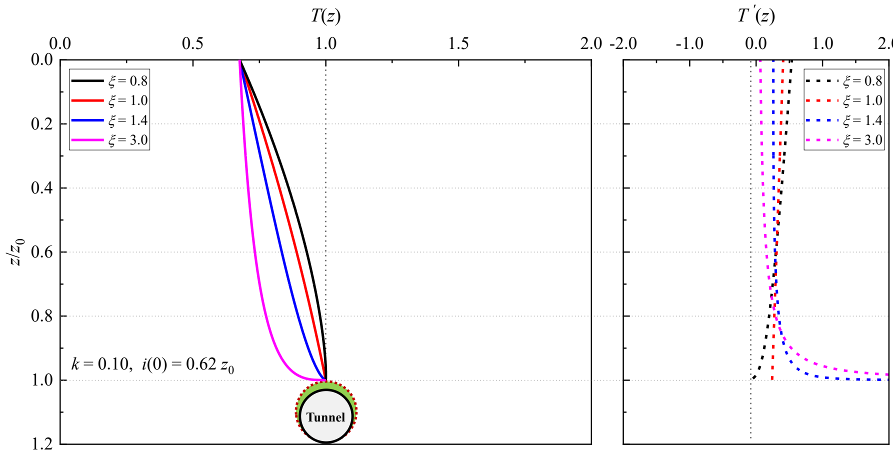

(b) effect of ξ with $T(0) > 1$

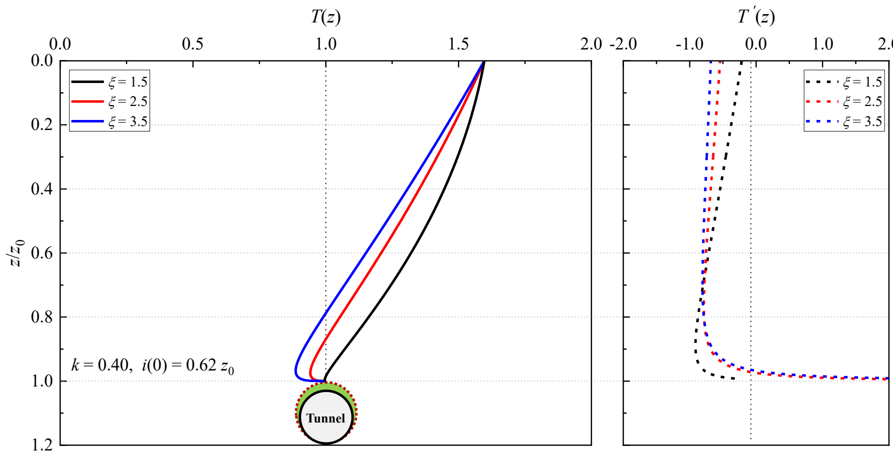

(c) effect of ξ with $T(0) < 1$

Fig. 3 Parameter effect on TRGVL and its first derivative.

3. Validation of TRGVL

A total of 8 field project cases and 7 model test cases are investigated to validate the formula of $T(z)$, and then, the volumetric deformation feature of the soil above the tunnel are analyzed in these cases.

3.1. Field project cases

For each field project case, basic information of the engineering, as well as the known quantities and parameters in the formula of $T(z)$ are listed in Table 1. In these cases, z_0, tunnel diameter D, $V_{l,r}$, $S_{max}(0)$ and $S_{max}(z_0)$ are directly obtained from the literature; parameter ξ is calibrated by the suggested method in Section 2.1.2, and parameter k is provided by literatures or calculated by the settlement trough widths at the ground surface and a certain depth. Data points that are used to calibrate ξ and k are circled in the corresponding figure for each case.

Table 1 Field project information and parameters of the formula $T(z)$.

Case No.	Project name	Tunnel information			Known quantities			Parameters		References
		z_0 (m)	D (m)	$V_{l,r}$ (%)	$S_{max}(z_0)$ (mm)	$S_{max}(0)$ (mm)	$i(0)/z_0$	k	ξ	
1	Interval tunnel of Tianjin Metro Line 1	8.65	6.40	/	200.00△	36.80	0.59	0.15	6.35	Li (2004)
2	Hyde Park tunnel (westbound tunnel)	30.65	7.10	0.78	27.74△△	5.67	0.42	0.23	5.15	Wan et al. (2017a)
3	Furongjiang tunnel	3.50	4.20	/	130.00△	26.84	0.82	0.25	4.62	Yi (1993)
4	Second Heinenoord tunnel	12.5	8.30	/	46.80☆	26.50	0.50	0.16	2.36	Federico et. al. (2014)
5	Thunder Bay tunnel	9.47	2.47	13.70	164.00△	46.90	0.40	0.35	6.00	
6	Green Park tunnel, U.K.	27.30	4.14	1.60	13.80△	6.10	0.50	0.33	2.14	
7	Rengent Park tunnel (North line)	17.90	4.42	1.30-1.40	17.00△	7.00	0.40	0.33	3.02	Loganathan et al. (1998)
8	Rengent Park tunnel (South line)	34.10	4.42	1.30-1.40	23.00△	5.60	0.27	0.22	3.72	

Note: △represents values of g provided by references; △△represents $S_{max}(z_0)$ calculated by Eq.(8); ☆represents $S_{max}(z_0)$ obtained by analytical method.

3.1.1 Interval tunnel of Tianjin Metro Line 1

Tianjin Metro Line 1 lies between Liuyuan and Shuanglin with a total length of 26.2 km, and consists of 26 subway stations. The interval tunnel from Xiaobailou station to Xiawafang station was excavated by an EPB (earth pressure balance) shield with a diameter of 6.4 m (Li, 2004). The depth of the tunnel axis is 11.85 m. Fig. 4(a) presents the soil profile in the site. The water level is 1.1 m below the ground surface.

Figs. 4(a) and (b) respectively present the measured maximum settlements and the measured settlement troughs at z = 0.0 m, 3.0 m, 5.0 m. Note that $S_{max}(z_0)$ is taken as the gap between the diameter of the excavation section and that of the lining. In Fig. 4(a), ξ is calibrated based the maximum settlements at the ground surface and the tunnel crown. In Fig.4(b), the circled data points at z = 0.0 m and 7.0 m are used to calibrate the Gaussian curves to obtain the values of $i(0)$ and $i(7)$, and then k is obtained by substituting $i(0)$ and $i(7)$ into Eq. (5).

Fig. 4(c) presents the measured and predicted results of $T(z)$. The measured results are obtained by using the area of the measured settlement trough dividing that of the settlement trough at tunnel crown in Fig. 4(b), wherein the measured settlement trough is obtained by connecting the measured settlement points using the Akima spline. The measured data indicates that $T(z)$ gradually decreases from the tunnel crown to ground surface, and the predicted curve of $T(z)$ can well capture this variation law, as shown in Fig.4(c). Meanwhile, the curve of $T'(z)$ is shown in Fig.4(d), which indicates that significant dilation occurs to the silt layer near the tunnel crown, and the upper silty clay and filling ground layers are approximately undrained. Besides, because more soil dilation usually means more ground disturbance during the tunnelling process, the disturbance degree of the silt layer is much larger than that of the upper layers in this case.

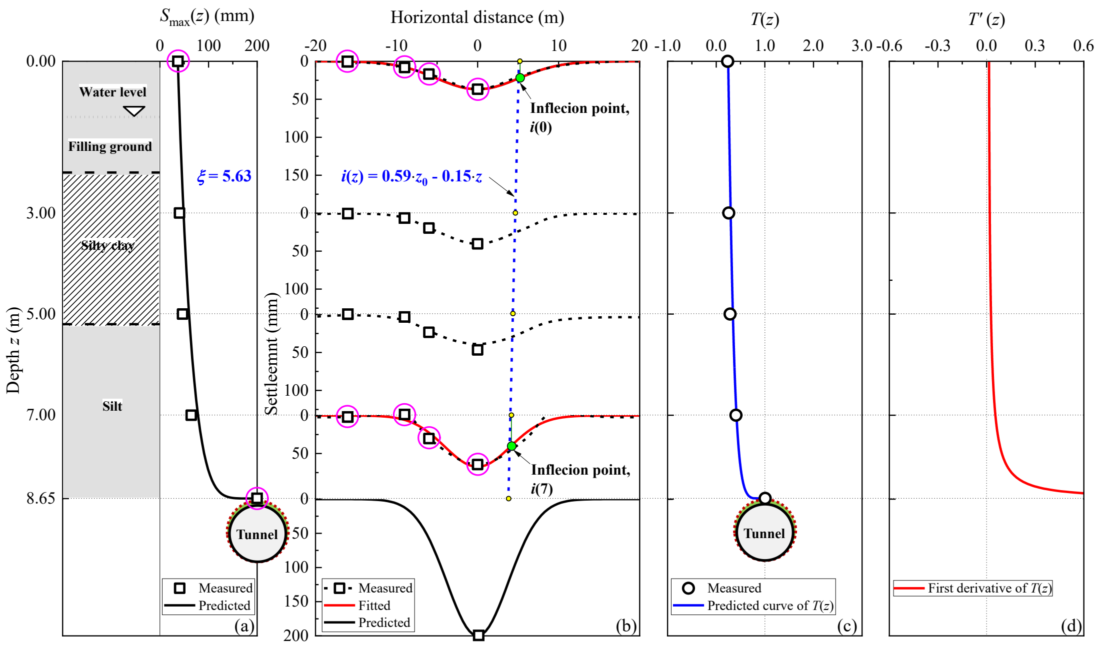

Fig. 4 Ground settlements and the TRGVL in interval tunnel from Xiaobailou to Xiawafang.

3.1.2 Hyde Park tunnel

Hyde Park tunnel was built beneath central London. The tunnels were excavated using the EPB shield with the diameter of 7.1 m. In this paper, ground settlements induced by the westbound tunnel excavation (Wan et al., 2017b) are collected to validate the formula for $T(z)$. The depth of the westbound tunnel axis is approximately 34.5 m. The soil profile in the site is presented in Fig. 5(a) (Wan et al., 2017a). The groundwater table is 4.6m below the surface.

The measured surface and subsurface settlements, together with the $S_{max}(z_0)$ provided by Lu et al. (2020a) are presented in Fig. 5(a) and (b). ξ is calibrated by Eq.(7), and k is calibrated based on the data points at z = 0.0 m and 26.0 m. Fig. 5(c) indicates that variation law of $T(z)$ in this case is similar to that in Case 1 and can be well described by the proposed formula. Fig. 5(d) indicates that the soil significantly dilates in the region that is 4.0 m higher above the tunnel.

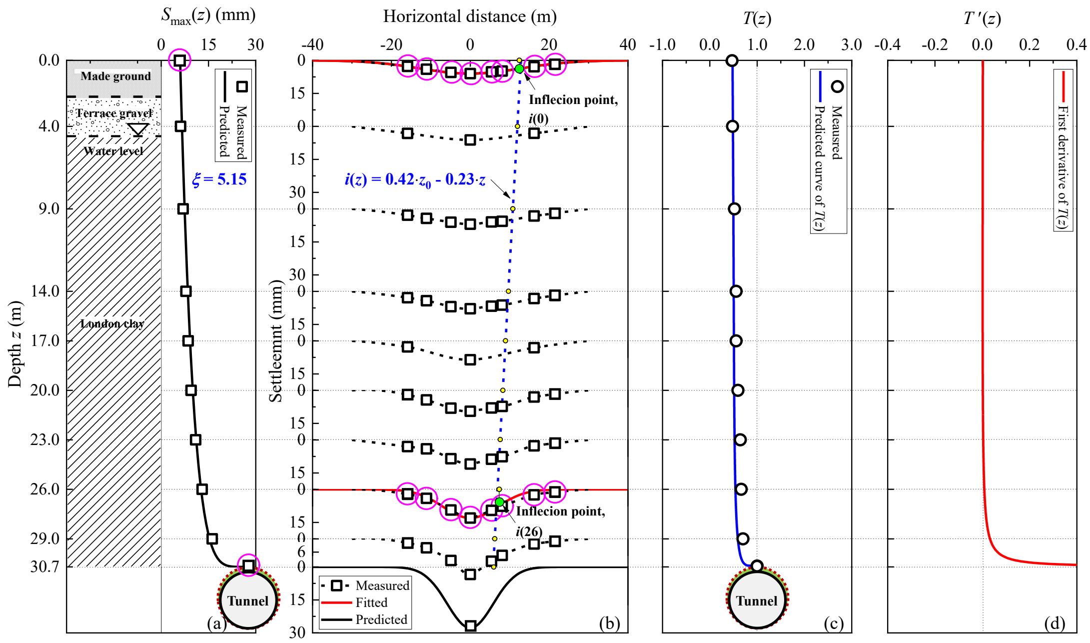

Fig. 5 Ground settlements and the TRGVL in Hyde Park tunnel.

3.1.3 Furongjiang sewer tunnel

Furongjiang sewer tunnel was excavated by an EPB shield with a diameter of 4.33 m in Shanghai. The outside diameter of the tunnel is 4.2 m, and the tunnel axis locates at 5.6 m below the ground surface. The groundwater table is 0.8 m in depth, and the soil profile is presented in Fig. 6(a) (Chen et al., 2011).

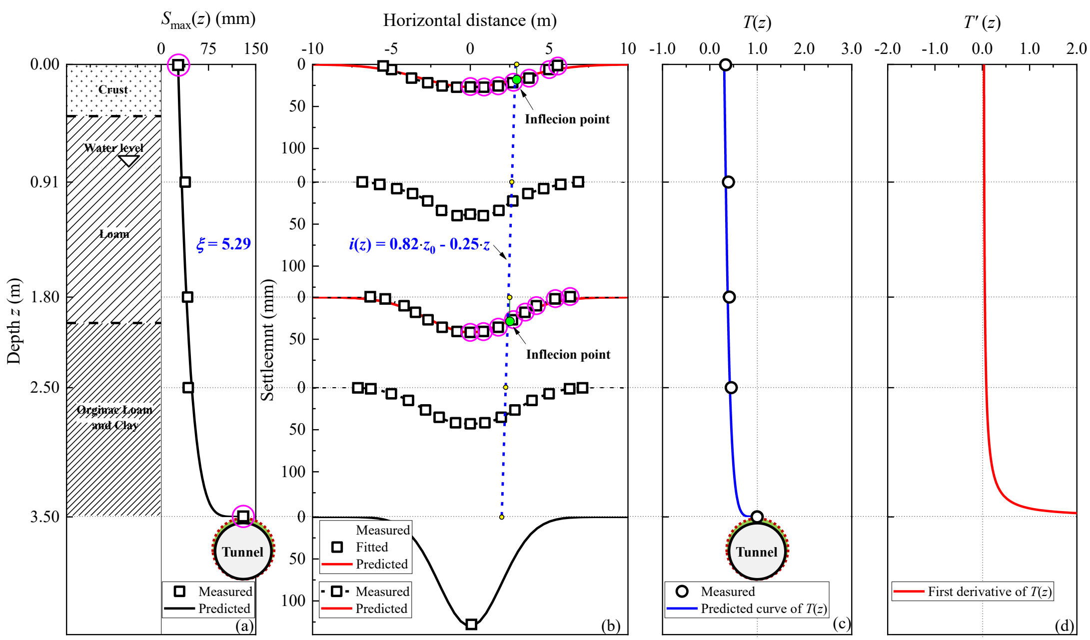

Fig. 6 Ground settlements and the TRGVL in Furongjiang sewer tunnel.

The measured maximum ground settlement and settlement troughs at different depth are presented in Fig. 6(a) and (b), respectively. Values of known quantities and parameters are listed in Table 1. The variation of $T(z)$ in this case is similar to that in Cases 1 and 2, as shown in Fig. 6(c). Fig. 6(d) indicates that the soil above the tunnel crown is disturbed more seriously.

3.1.4 Second Heinenoord tunnel

The Second Heinenoord tunnel, which passes under the Oude Maas river, Rotterdam, Netherlands, was excavated by shield. The outer diameter of the lining is 8.3 m, and the depth of its spring line is 16.65 m. The soil profile at the measured section comprises is presented in Figs. 7(a). The average groundwater table is 3.0 m below the ground surface (Federico et al., 2014).

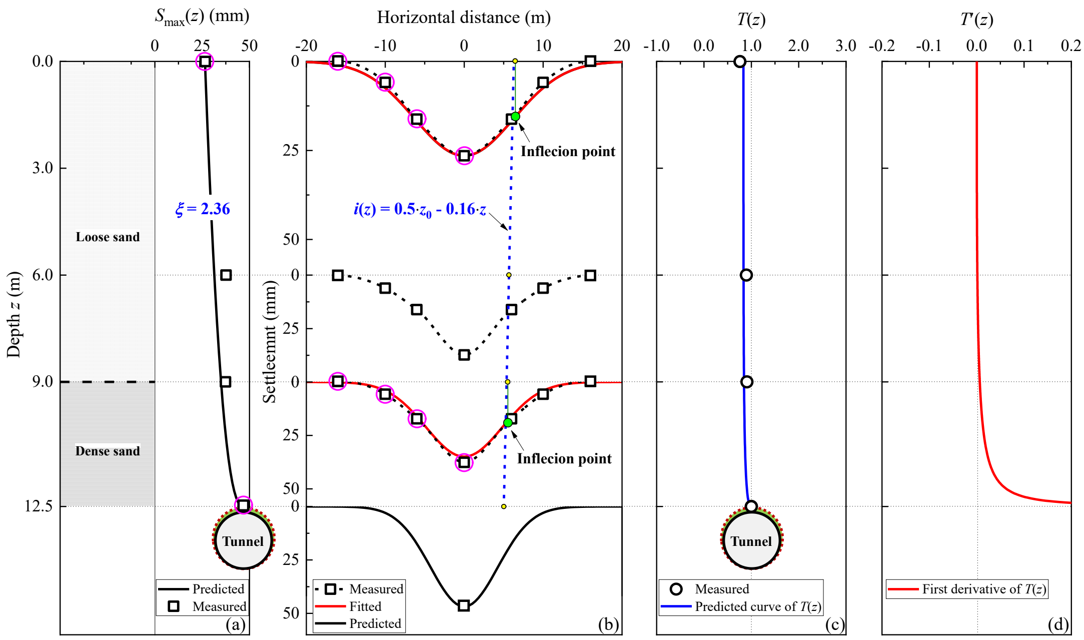

Fig. 7 Ground settlements and the TRGVL in the Second Heinenoord tunnel.

The measured settlements at the surface and subsurface, together with the $S_{max}(z_0)$ provided by Federico et al. (2014), are presented in Figs. 7(a) and (b). Fig. 7(c) indicates that there is a good correlation between the predicted and measured $T(z)$. In this case, the values of $T(z)$ change slowly with z compared with Cases 1~3. The curve of $T'(z)$ in Fig. 7(d) indicates that dilation mainly occurs to the dense sand layer near the tunnel crown, while the volume of the loose sand layer hardly changes.

3.1.5 Thunder Bay Tunnel

A sanitary trunk sewer tunnel, with a diameter of 2.47 m, was constructed by the tunnel boring machine in Thunder Bay, Ontario, Canada. The axis depth of the tunnel is 10.71 m. Loganathan et al. (1998) suggested that the excavation section volume loss is taken as 14.0%. A simplified soil profile is shown in Fig. 8(a).

Figs. 8(a) and (b) present the measured maximum settlements and settlement troughs, respectively, as well as the $S_{max}(z_0)$ provided by Lu et al. (2020a). Fig. 8(c) shows the measured and predicted results of $T(z)$. The measured results indicate that $T(z)$ decreases from the ground surface to the depth of 6.0 m. The predicted curve well captures the measured data points and shows the $T(z)$ first decreases and then increases from the tunnel crown to the ground surface. Fig. 8(d) indicates that the soil dilates only in a very small region near the tunnel crown, while contracts at the upper position. Considering the tunnelling method, we can infer that a large amount of water in the silty sand layer have been expelled from during the excavation process, so that the settlement degree of soil at upper position is larger.

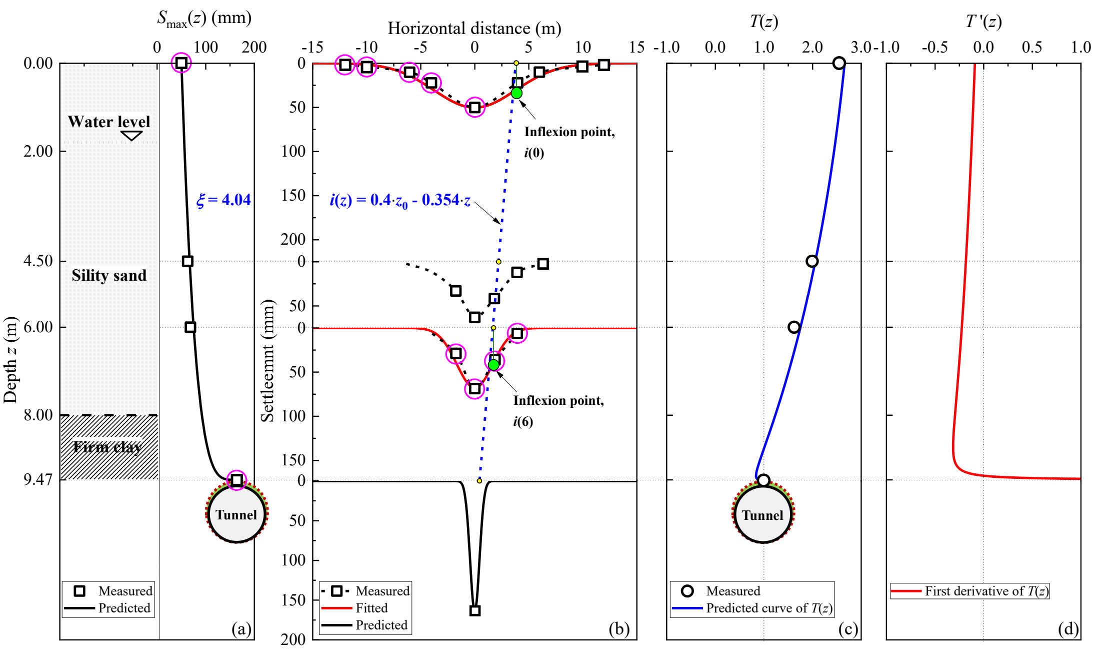

Fig. 8 Ground settlements and the TRGVL in Thunder Bay Tunnel.

3.1.6 Green Park tunnel

The Green Park tunnel, with a diameter of 4.14 m, was constructed by a hand-excavated shield at a depth of approximately 29.0 m in London. The simplified soil profile of the construction site is shown in Fig. 9(a). The underground water level was found at a depth of approximately 2.0 m (Attewell and Farmer, 1974).

For this case, ξ is determined by the proposed method, and k as well as the known quantities $S_{max}(0)$, $S_{max}(z_0)$, and $i(0)$ are provided by references (Chou and Bobet., 2002., Mair et al., 1993), as listed in Table 1. Figs. 9(c) and 9(d) indicates that curves of $T(z)$ and $T'(z)$ in this case are similar with that in Case 4. The different with Case 4 is that the volume of the soil within 9.0 m above the tunnel does not change as a whole, and that the soil significantly dilates with 1.0 m above the tunnel. Because both of the parameters and known quantities are reliable, it can be concluded that the predicted law of $T(z)$ is reasonable in this case although the measured results are not provided to validate the prediction result.

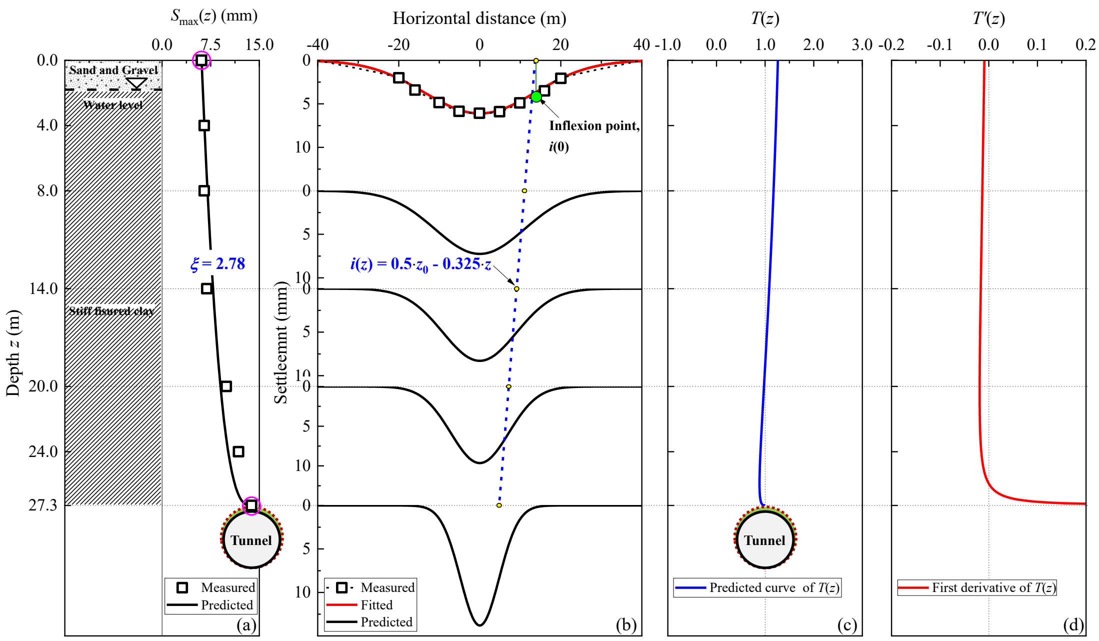

Fig. 9 Ground settlements and the TRGVL in Green Park tunnel.

3.1.7 Regent Park tunnel

Two tunnels, with their diameter being 4.42 m, were constructed at depths of 20.1 m (north line) and 34.1 m (south line) at Regent Park, London. The vertical distance between the tunnel centerlines is 14.0 m, and the horizontal distance is 18.0 m. Both tunnels were built by hand-excavated shield, and the south line was constructed first. The tunnels were excavated in London clay. The groundwater table was found at a depth of approximately 4.0 m. The ground volume loss ratio at the excavation section for both tunnels was 1.3-1.4% (Chou and Bobet., 2002).

Compared with case 8, the depth of tunnel in case 7 is shallower, so its settlement trough width is narrower, and the value of surface settlement is larger. On the other hand, the measured surface settlement presents slightly asymmetric distribution in case 7. The reason of asymmetric distribution is not explained in the literature. he author thinks that it may be caused by some random factors of the engineering. The measured surface settlement is used to determine $i(0)$, so the asymmetric distribution of surface subsidence has a certain influence on the prediction result of $T(z)$. In case 7, the asymmetric distribution of the surface settlement is so lightly, that is has little effect on the prediction results of $T(z)$. If the measured surface settlement has significant asymmetric distribution in an engineering case, we should analyze the specific reasons and exclude the data with large error to obtain a more appropriate value of $i(0)$.

For Cases 7 and 8, the way to obtain parameters and known quantities is the same as that in case 5, except for the $S_{max}(z_0)$, as shown in Figs. 10(a)~(b) and Figs. 11(a)~(b). $S_{max}(z_0)$ is calculated using Eq. (8) with $V_{l,r}$ = 1.3%. The predicted curves of $T(z)$ are respectively presented in Figs. 10(c) and Fig. 11(c), and the corresponding $T'(z)$ are presented in Figs. 10(d) and Fig. 11(d). It can be seen that variation of $T(z)$ and $T'(z)$ in Case 6 and Case 7 are basically same as that in Case 4 and Case 5, respectively. In these two cases, the measured results of $T(z)$ also cannot be provided, but the rationality of the predicted law can be proved by the reliable parameters and known quantities.

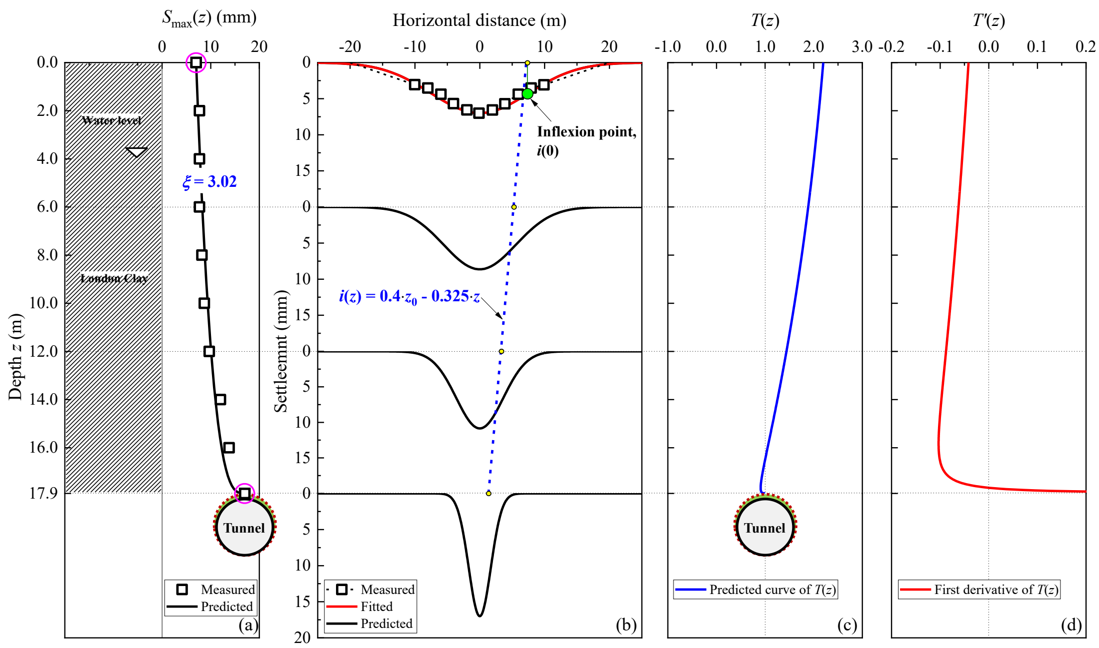

Fig. 10 Ground settlements and the TRGVL in Regent Park tunnel (North Line).

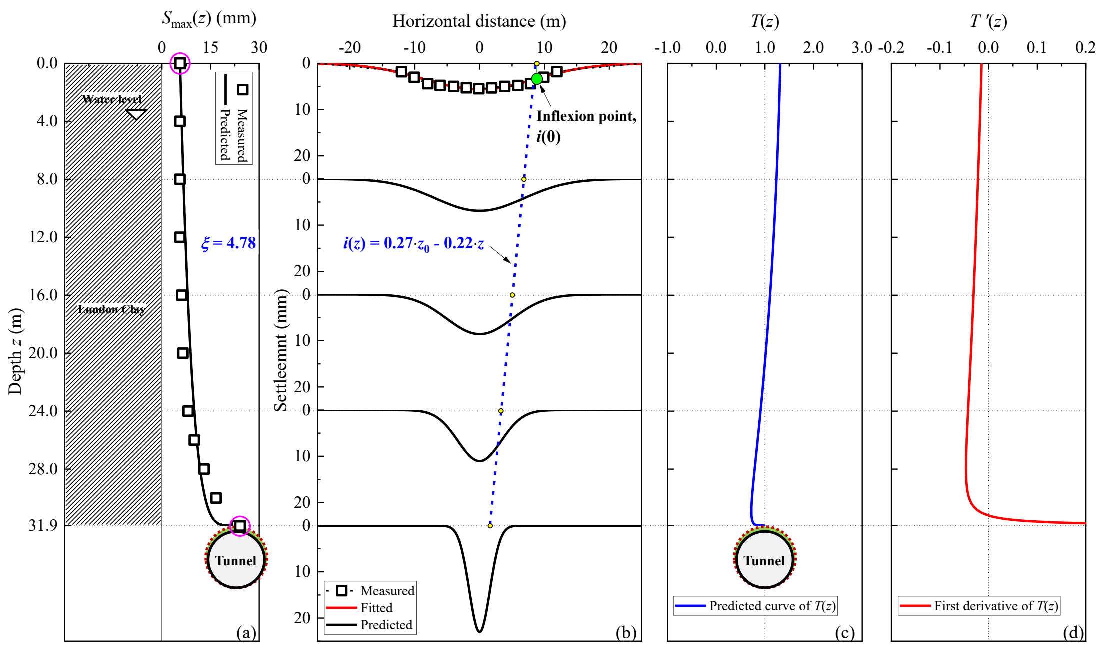

Fig. 11 Ground settlements and the TRGVL in Regent Park tunnel (South line).

3.2. Model test cases

Two model tests of tunnel excavation are collected to further validate the proposed formula of $T(z)$, and the application and limitation of the formula are clarified. Known quantities and parameters needed by $T(z)$ corresponding to each test condition are listed in Table 2. In these cases, known quantities are directly obtained from the literature, and parameters k and ξ are calibrated on the basis of the data points circled in the corresponding figure.

Table 2 Model test information and parameters of the formula $T(z)$.

Case No.	Project name	Tunnel information			Known quantities			Parameters		References
		z_0 (cm)	D (cm)	$V_{l,r}$ (%)	$S_{max}(z_0)$ (mm)	$S_{max}(0)$ (mm)	$i(0)/z_0$	k	ξ	
9	Centrifuge tests	15.1	6.2	0.50	0.10	0.097	0.60	0.44	2.51	Marshall (2009)
10				1.00	0.25	0.193	0.60	0.35	2.49	
11				2.50	0.60	0.367	0.62	0.40	2.35	
12	1g model tests	50.0	20.0	0.66	0.32	0.140	0.14	0.02	2.25	Pan (2015)
13				1.97	0.70	0.180	0.14	0.02	2.10	
14				3.29	1.98	0.350	0.14	0.02	1.17	
15				5.26	3.02	1.020	0.14	0.02	0.65	

3.2.1 Centrifuge test cases

A group of centrifuge tests about tunnel excavation, with $V_{l,r}$ as the only variable controlled, were conducted by Marshall (2009). The acceleration is 75g. $V_{l,r}$ is controlled by extracting fluid from the model tunnel, and equal to 0.5%, 1.0%, 2.5%, and 5.0%, respectively. The tunnel diameter is 6.2 cm, and the depth of the tunnel axis is 18.2 cm. Dry silica sand known as Leighton Buzzard Fraction E is used for testing. Relative density of the sand is 90%, and the unit weight is 15.65 kN/m^3. When $V_{l,r}$ reaches 5.0%, the sand collapses above the tunnel crown and the stable soil arch forms in the test model. Distribution of the measured $S_{max}(z)$ appears to be S-shape at this moment, so that the proposed formula for $T(z)$ is no longer applicable. Therefore, test results corresponding to $V_{l,r}$ = 0.5%, 1.0%, and 2.5% are presented in this section, as shown in subfigure (a) and (b) of Figs. 12~14.

The measured and predicted $T(z)$ in three conditions are respectively presented in the subfigure (c) of Fig. 12~14, and good agreement can be found. When $V_{l,r}$ = 0.5%, $T(z)$ increases monotonously from the tunnel crown to the ground surface (Fig. 12(c)). When $V_{l,r}$ increases to 1.0%, however, there is a slight tendency of decreasing for $T(z)$ at the tunnel crown (Fig. 13(c)). This tendency becomes more obvious when $V_{l,r}$ = 2.5% (Fig. 14(c)), which indicates that the dilation degree of soil is strengthened with the increase of $V_{l,r}$. The curves of $T'(z)$ in Figs. 12(d), 13(d) and 14(d) can also interpret this variation.

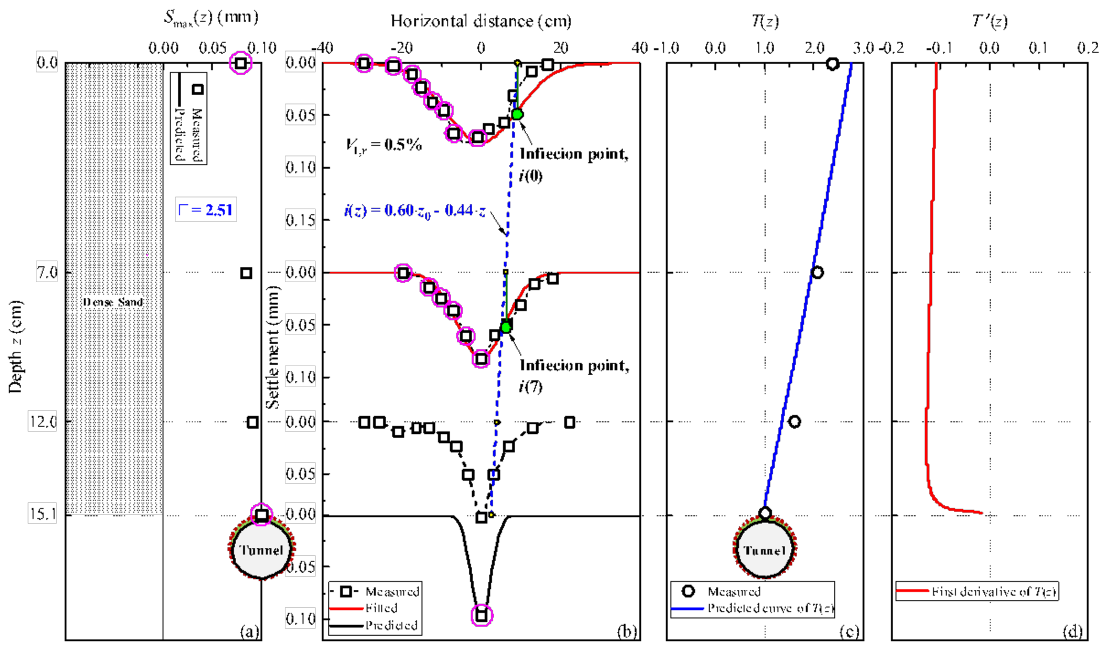

Fig. 12 Ground settlements and the TRGVL when $V_{l,r}$ = 0.5% in Marshall's test.

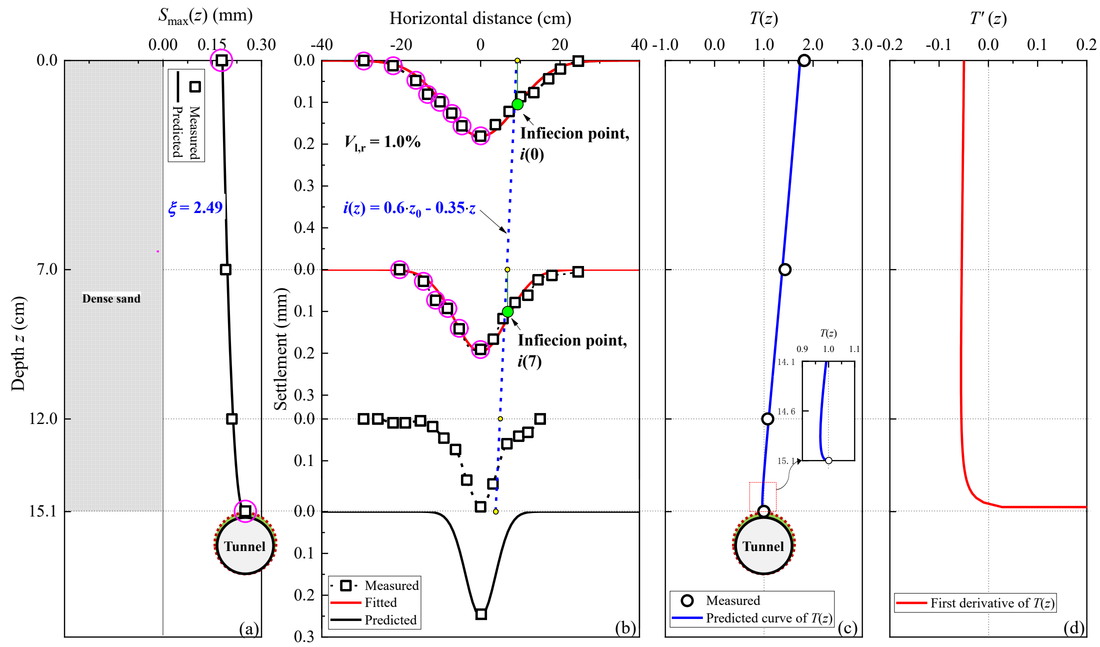

Fig. 13 Ground settlements and the TRGVL when $V_{l,r}$ = 1.0% in Marshall's test.

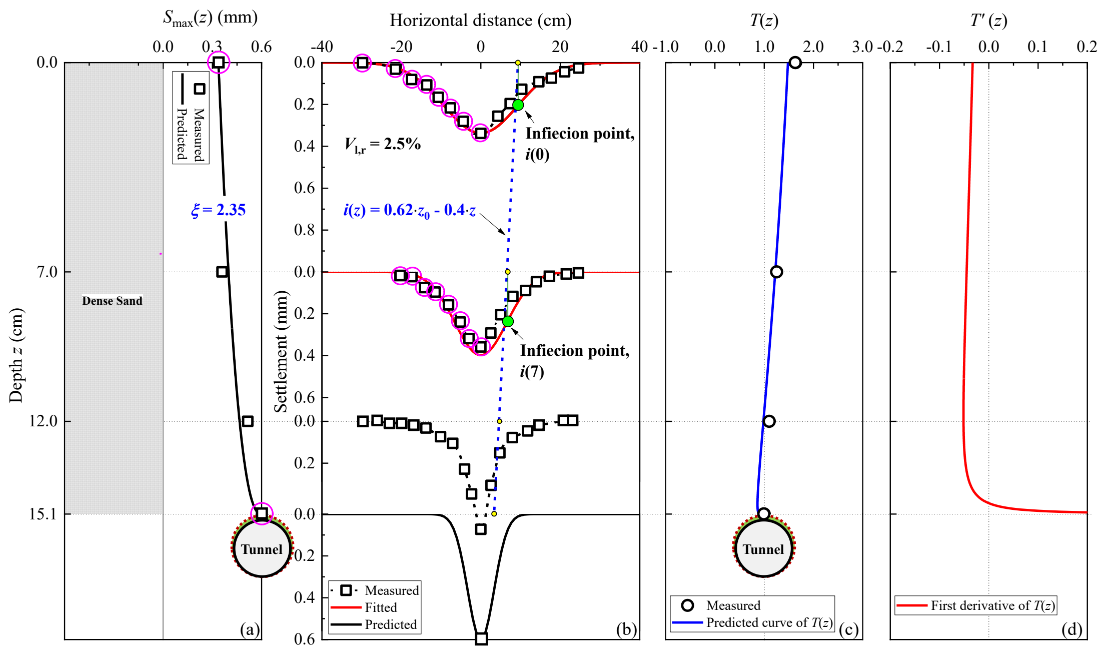

Fig. 14 Ground settlements and the TRGVL when $V_{l,r}$ = 2.5% in Marshall's test.

3.2.2 1g model tests

Pan (2015) conducted a group of 1g model tests of tunnelling, in which tunnel excavation was achieved by expelling water. The model tunnel has a diameter of 20 cm, and its axis is in the depth of 60 cm. $V_{l,r}$ is the single variable controlled in the test, and is equal to 0.66%, 1.97%, 3.29%, and 5.26%, respectively. Silica sand, with an initial void ratio of 0.65, is used for testing. The unit weight of the soil is approximately 16.67 kN/m^3. In the test, the soil near the tunnel began to collapse when $V_{l,r}$ = 3.29%, and the collapse developed to the ground surface when $V_{l,r}$ = 5.26%. The measured settlements corresponding to each $V_{l,r}$ are presented in the subfigures (a) and (b) of Figs. 15~18.

From subfigures (c) of Figs. 15~18, it can be found that $T(z)$ monotonously decreases from the tunnel crown to the ground surface in all the four test conditions. However, the decrease rate of $T(z)$ gradually becomes slow when $V_{l,r}$ = 0.66% and 1.97% (Figs.15(c) and 16(c)), while $T(z)$ decreases in an approximately constant speed when $V_{l,r}$ = 3.29% (Fig.17(c)), and in an accelerated speed when $V_{l,r}$ = 5.26% (Fig.18(c)). When $V_{l,r}$ = 5.26%, the soil near the tunnel crown collapses so seriously that the dilation degree of the soil reaches the maximum in this region, which can reasonably explain the variation of $T(z)$ in this test condition, as shown in Fig. 18(d).

Meanwhile, the predicted curves of $T(z)$ are also presented, as shown in figures (c) of Figs. 15~18. k is calibrated by substituting $i(0)$ and $i(20)$ into Eq. (5) for each case. ξ is calibrated by Eq. (8) when $V_{l,r}$ = 0.66% and 1.97%, but is determined by fitting the measured $S_{max}(z)$ using Eq. (6) when $V_{l,r}$ = 3.29%, and 5.26%. Comparison between the predicted and measured results of $T(z)$ indicates that the suggested method can well describe the variation of $T(z)$ in this test, even if the soil above the tunnel has significantly collapsed.

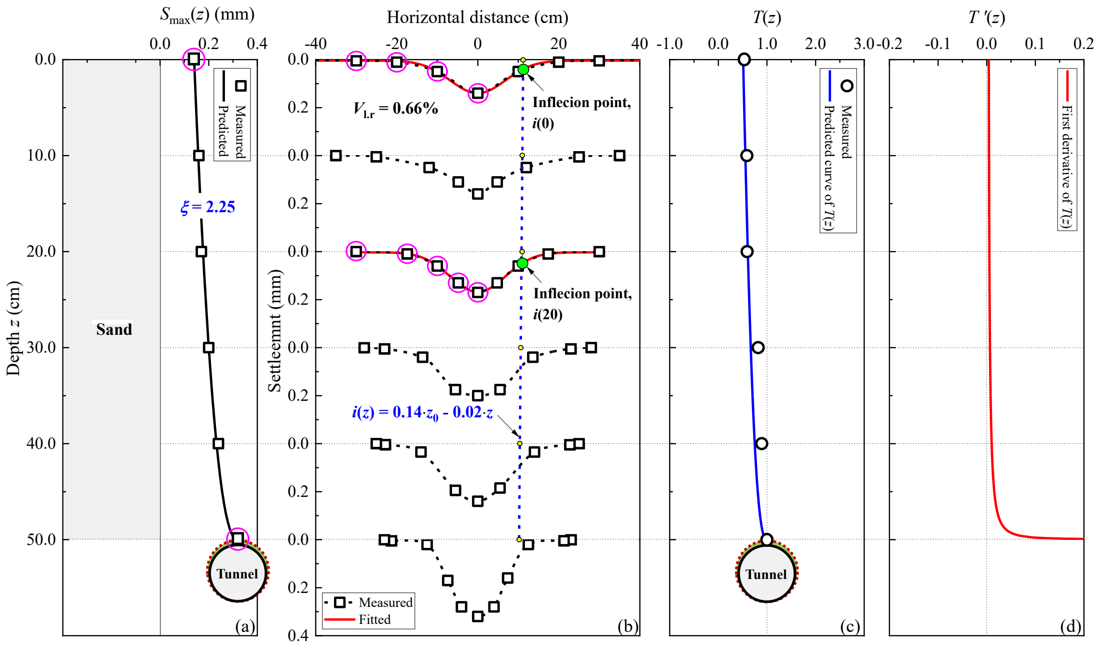

Fig. 15 Ground settlements and the TRGVL when $V_{l,r}$ = 0.66% in Pan's test.

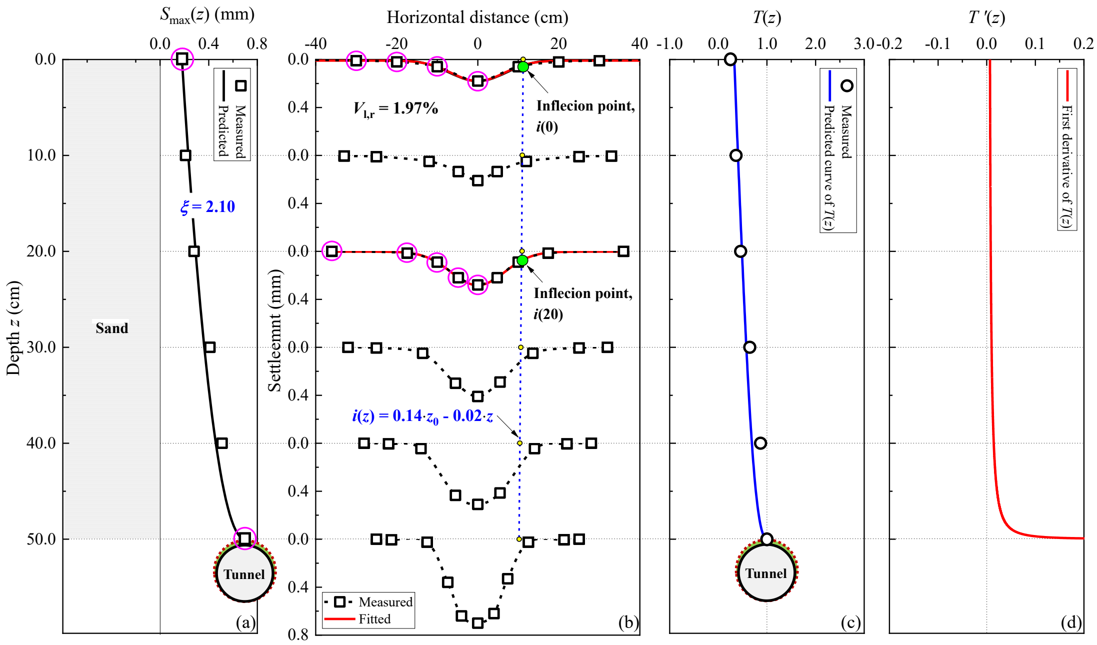

Fig. 16 Ground settlements and the TRGVL when $V_{l,r}$ = 1.97% in Pan's test.

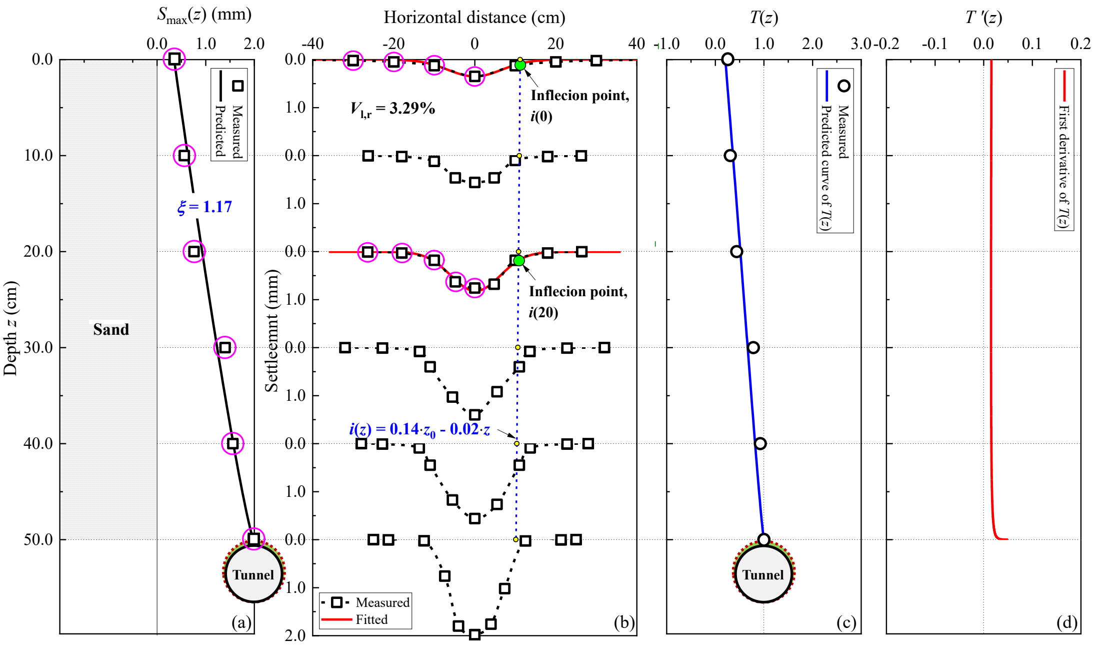

Fig. 17 Ground settlements and the TRGVL when $V_{l,r}$ = 3.29% in Pan's test.

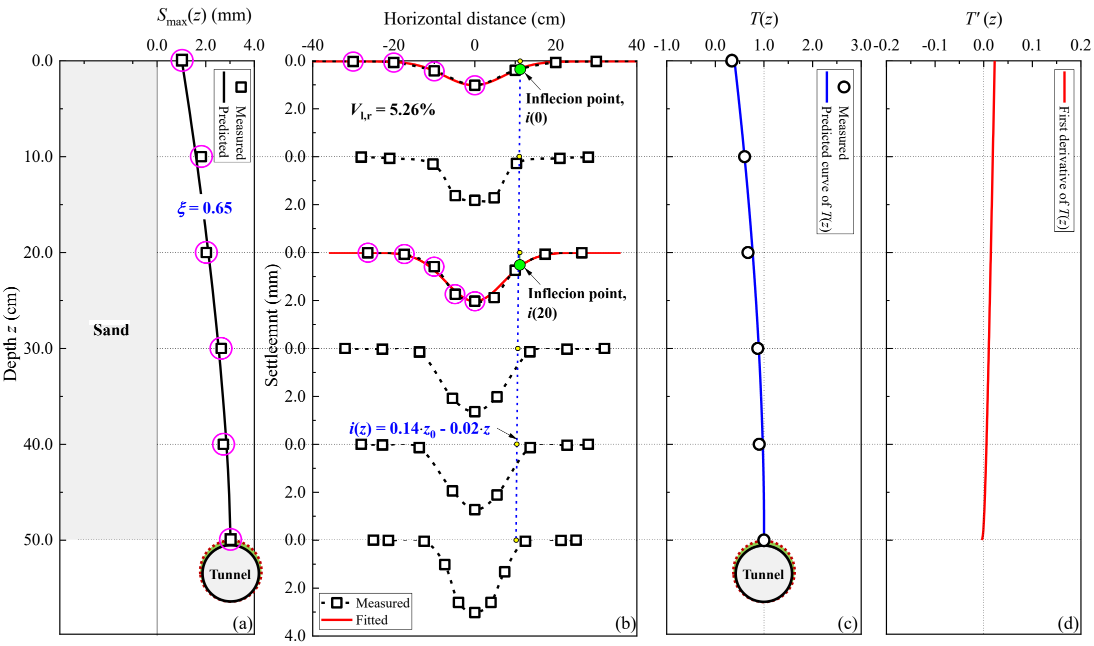

Fig. 18 Ground settlements and the TRGVL when $V_{l,r}$ = 5.26% in Pan's test.

4. Further discussion on TRGVL

$T(z)$ reflects the overall volumetric deformation of the soil between the tunnel crown and depth z, while $T'(z)$ can be used to judge the contraction/dilation behaviour of the soil at depth z. In the above cases, variation of $T(z)$ from the tunnel crown to the ground surface shows the following four modes.

Form **A**, corresponding to Case 9, is illustrated in Fig. 19(a). In this form, $T(z)$ gradually increases, and $T'(z)$ is always negative, which means that the soil at any depth shows volumetric contraction. The soil above the tunnel becomes denser, and it is disturbed slightly.

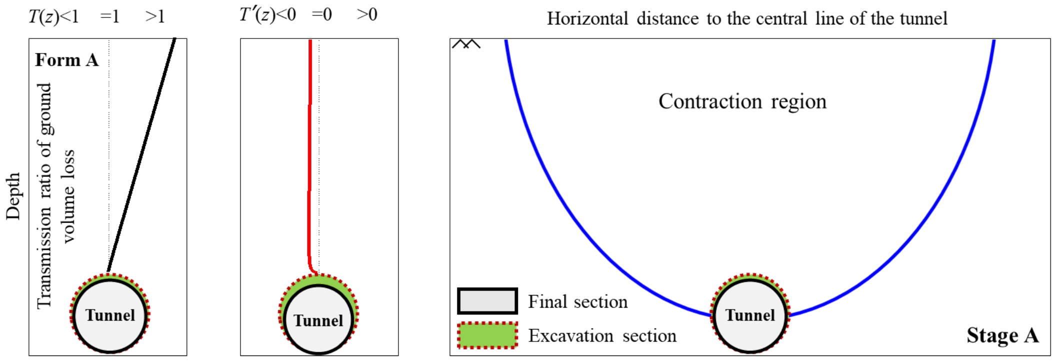

(a) Low excavation section volume loss

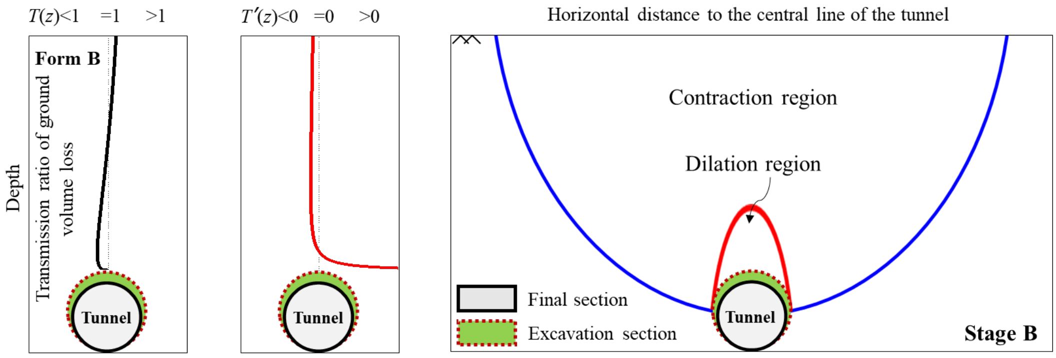

(b) Medium excavation section volume loss

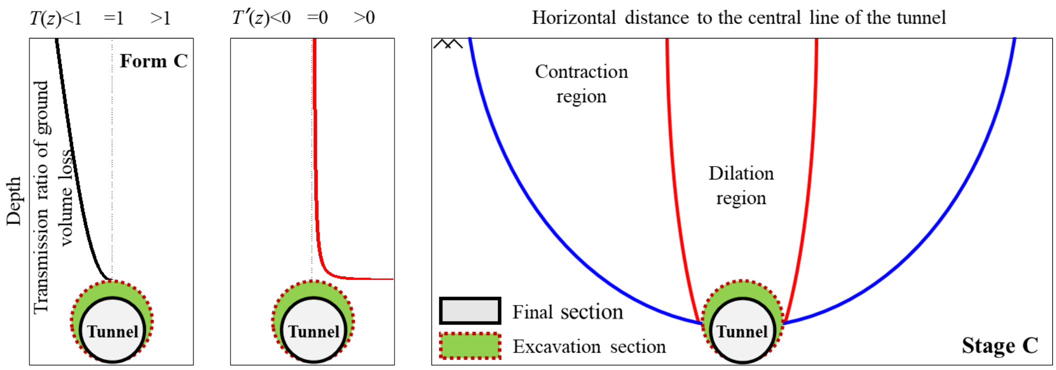

(c) High excavation section volume loss

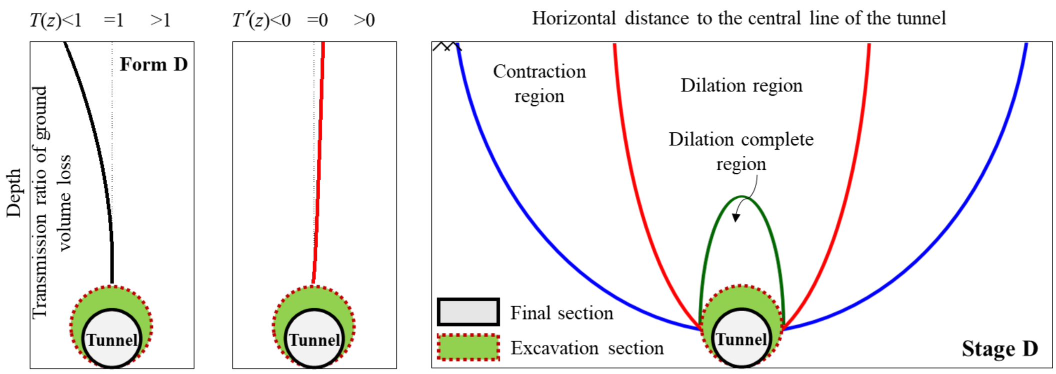

(d) Extremely high excavation section volume loss

Fig. 19 Variation forms of $T(z)$ and the corresponding volumetric deformation feature.

Form **B**, corresponding to Cases 5, 6, 7, 8, 10, and 11, is illustrated in Fig. 19(b). $T(z)$ first decreases and then increases, and $T'(z)$ is positive near the tunnel crown and negative near the ground surface, indicating that the soil turns from dilative to contractive as z decreases. The soil is disturbed in a region near the tunnel crown because it becomes loose in this region.

Form **C**, corresponding to Cases 1, 2, 3, 4, 12, 13, and 14, features a decreasing $T(z)$ in an accelerated speed, as shown in Fig. 19(c). $T'(z)$ is positive at any depth above the tunnel, and its value is the largest at the tunnel crown. Therefore, the soil above the tunnel exhibits volumetric dilation. In this condition, the disturbed region expands to the ground surface. The disturbance degree of the soil gradually decreases as z decreases.

Form **D**, corresponding to Case 15, also exhibits a decreasing $T(z)$ but its speed gradually slows down, as illustrated in Fig. 19(d). The value of $T'(z)$ in Form **D** is almost 0 in a region above the tunnel crown, which indicates the soil volume in this region does not change. The only possibility corresponding to this condition is that the soil collapses as a whole.

In a tunnel project, variation of $T(z)$ will evolve from Form **A** to Form **D** as $V_{l,r}$ increases, since the development of the volumetric deformation of the soil above the tunnel goes through four stages in turn, i.e., Stage A ~ Stage D, as shown in Fig. 19. When $V_{l,r}$ is very small, the soil at any depth above the tunnel contracts, i.e., Stage A. As $V_{l,r}$ increases, dilation occurs in the soil near the tunnel crown i.e., Stage B, and the dilation region gradually expands to the ground surface i.e., Stage C. During this process, $T(z)$ first develops from Form **A** to Form **B**, then to Form **C**. When $V_{l,r}$ increases to an extremely high value, the soil above the tunnel collapses, and the collapsed soil moves downward as a whole i.e., Stage D. If the collapse can extend to the ground surface, the volume increment of the soil at the upper position is more than that at the lower position, so variation of $T(z)$ is like Form **D**. If a stable soil arch, which prevents the collapse to develop to the ground surface, can be formed in the ground, the soil usually dilates between the soil arch and the tunnel crown, but contracts or dilates near the ground surface. The evolution of $T(z)$ stops at Form **B** or Form **C**.

For a field tunnel project, the value of $V_{l,r}$ gradually increases and reaches a fixed value in a transverse section during the tunnelling process, so $T(z)$ evolves from Form **A** to one of these four forms. When $T(z)$ always appears as Form **A** or **B**, the soil above the tunnel is stable, and maintaining the current construction method can ensure the safety of tunnel construction. When $T(z)$ develops to Form **C**, the engineers should pay close attention to the soil near the tunnel crown to judge whether the soil will collapse or not. If $T(z)$ gradually evolves from Form **C** into the Form **D**, the soil above the tunnel will collapse, as demonstrated by the test of Pan (2015). During the process, $T'(z)$ changes from a large positive value to almost 0 in a region near the tunnel crown, as shown in Fig. 19(c) and (d). When this phenomenon occurs, reinforcement measures need to be conducted to prevent the collapse of the soil above the tunnel.

5. Conclusions

Based on the developed Gaussian function, this work presents the formula for transmission ratio of ground volume loss (TRGVL), which can be used to describe the variation of the ground volume loss with depth quantificationally. The soil volume change is the reason why the ground volume loss varies with depth, so the first-order derivative of TRGVL essentially reflects the volumetric deformation of the soil at a certain depth. The soil dilates when the first-order derivative of TRGVL is positive and contracts in the opposite condition. More dilation makes the soil looser, so that the disturbance degree induced by tunnelling is larger. The disturbance degree of the soil above the tunnel can be evaluated by the TRGVL and its first-order derivative.

The data from field projects and model tests indicates that, from the tunnel crown to ground surface, variation of TRGVL presents as four forms, i.e., **A** gradually increasing; **B** first decreasing and then increasing; **C** decreasing in a decelerated speed; **D** decreasing in an accelerated speed. When TRGVL evolves form Form **A** to Form **C**, the disturbance range and degree of the soil above the tunnel increases gradually, but collapse dose not occur during this process. When TRGVL evolves from Form **C** into the Form **D**, the soil above the tunnel will collapse, and enforcement measures need to be conducted. The proposed TRGVL can be used as a new index to evaluate the disturbance degree of the soil above the tunnel.

Declaration of Competing Interest

The authors declare that they have no known competing financial interests or personal relationships that could have appeared to influence the work reported in this paper.

Acknowledgements

The authors gratefully acknowledge financial support from the National Outstanding Youth Science Fund Project of National Natural Science Foundation of China (Grant No. 52025084) and the National Natural Science Foundation of China (Grant Nos. 51538001; 51778026).

Notation:

D	excavation diameter of the tunnel
$i(z)$	settlement trough width coefficient at a depth of z
k	slope of $i(z)$
$S_{\max}(z)$	maximum settlement at depth z
V_l	ground volume of the tunnel excavation section
$V_{l,r}$	ground volume loss ratio of the tunnel excavation section
$V_l(z)$	ground volume loss at depth z
$T(z)$	Transmission ratio of the ground volume loss at depth z
z_0	depth of the tunnel crown
z	depth, measured from ground surface
ξ	parameter used in empirical formulas of $S_{\max}(z)$

REFERENCES

[1] Atkinson JH, Potts DM. Subsidence above shallow tunnels in soft ground. ASCE Journal of Geotechnical Engineering Division 1977;103(4):307-325.

[2] Attewell PB, Farmer IW. Ground deformations resulting from shield tunnelling in London Clay. Canadian Geotechnical Journal 1974;11(3): 380-395.

[3] Boonsiri I, Takemura J. Ittichai B, Jiro T. Observation of ground movement with existing pile groups due to tunneling in sand using centrifuge modelling. Geotechnical and Geological Engineering 2015; 33:621-640.

[4] Celestino TB, Gomes RAMP, Bortolucci AA. Errors in ground distortions due to settlement trough adjustment. Tunneling and Underground Space Technology 2000; 15(1): 97-100.

[5] Chen RP, Zhu J, Liu W, Tang XW. Ground movement induced by parallel EPB tunnels in silty soils. Tunnelling and Underground Space Technology 2011; 26(1):163-171.

[6] Dong XJ, Karrech A, Qi CC, Elchalakani M, Basarir H. Analytical solution for stress distribution around deep lined pressure tunnels under the water table. International Journal of Rock Mechanics and Mining Sciences 2019: 104124.

[7] Fang Q, Liu X, Zhang DL, Lou HC. Shallow tunnel construction with irregular surface topography using cross diaphragm method. Tunnelling and Underground Space Technology 2017; 68, 11-21.

[8] Fang YS, Wu CT, Chen SF. An estimation of subsurface settlement due to shield tunneling. Tunnelling and Underground Space Technology 2012; 44:121-129.

[9] Federico P, Despina M, Zymnis, SM, Andrew JW. Ground movements due to shallow tunnels in soft ground. II: Analytical interpretation and prediction. ASCE Journal of Geotechnical and Geoenvironmental Engineering 2014; 140(4): 04013041.

[10] Franza A. Tunnelling and its effects on piles and piled structures. PhD thesis, University of Nottingham; 2017.

[11] Hu XY, Yan QX, He C, Yang XY. Study on the disturbance and excavation face failure feature of granular mixtures stratum due to EPB shield tunneling. Chinese Journal of Rock Mechanics and Engineering 2016; 35(8): 1618-1627.

[12] Ieronymaki ES, Whittle AJ, Einstein HH. Comparative study of the effects of three tunneling methods on ground movements in stiff clay. Tunnelling and Underground Space Technology 2018; 74(4):167-177.

[13] Jiang YC, He C, Hu XY, Fang Y. Laboratory test study of soil disturbance caused by shield tunnelling in sandy strata. Chinese Journal of Rock Mechanics and Engineering 2013; 32(12):2550-2559.

[14] Lee KM, Rowe RK, Lo KY. Subsidence owing to tunneling. I. Estimating the gap parameter. Canada Geotechnical Journal 1992; 29(6), 929-940.

[15] Lee YJ. Investigation of subsurface deformations associated with model tunnels in a granular mass. Tunnelling and Underground Space Technology 2009; 24(6): 654-664.

[16] Li Y. The 3D FEM simulation and experimental research on ground deformation by shield driven. PHD Thesis, Tianjin University; 2004.

[17] Loganathan N, Poulos HG. Analytical prediction for tunneling induced ground movement in clays. ASCE Journal Geotechnical and Geoenvironmental Engineering 1998; 124(9):846-856.

[18] Lu DC, Lin QT, Tian Y, Du XL, Gong QM. Formula for predicting ground settlement induced by tunnelling based on Gaussian function. Tunnelling and Underground Space Technology 2020a; 103: 103443.

[19] Lu DC, Kong FC, Du XL, Shen CP, Gong QM, Li PF. A unified displacement function to analytically predict ground deformation of shallow tunnel. Tunnelling and Underground Space Technology 2019; 88: 129-143.

[20] Lu DC, Kong FC, Du XL, Shen CP, Su CC, Wang J. Fractional viscoelastic analytical solution for the ground displacement of a shallow tunnel based on a time-dependent unified displacement function. Computers and Geotechnics 2020b; 117: 103284.

[21] Mahmoud A, Magued I. Analysis of Tunneling-Induced Ground Movements Using Transparent Soil Models. Journal of Geotechnical and Geoenvironmental Engineering (ASCE) 2011; 137(5): 525-535.

[22] Mair RJ, Taylor RN, Bracegirdle A. Subsurface settlement profiles above tunnels in clays. Géotechnique 1993;

43(2):315-320.

[23] Mair RJ, Taylor RN. Bored tunnelling in the urban environment. In: Proceeding of the 14th International Conference of Soil Mechanics and Foundation Engineering, Hamburg, UK; 1997.

[24] Marshall AM. Tunnelling in sand and its effect on pipelines and piles. PhD thesis, University of Cambridge; 2009.

[25] Marshall AM, Farrell R, Klar A, Mair RJ. Tunnels in sands: the effect of size, depth and volume loss on greenfield displacements. Géotechnique 2012; 62(5): 385-399.

[26] Peck RB. Deep excavations and tunnelling in soft ground. In: Proceedings of the 7th International Conference on Soil Mechanics and Foundation Engineering, State of the Art Volume, Mexico; 1969.

[27] Pan ZG. Study on the ground deformation of soil tunnel excavation. PhD thesis, Beijing University of Technology; 2015.

[28] Vorster TE, Klar A, Soga K, Mair RJ. Estimating the effects of tunneling on existing pipelines. Journal of Geotechnical and Geoenvironment Engineering 2005;131(11): 1399-1410.

[29] Wang F, Miao LC, Yang XM, Du YJ, Liang FY. The volume of settlement trough change with depth caused by tunneling in sands. KSCE Journal of Civil Engineering 2016; 20(7): 2719-2724.

[30] Wang J，He C，Hu RQ，Dai GH，Wang SM. Soil disturbance induced by EPB shield tunnelling in upper-soft and lower-hard ground. Chinese Journal of Rock Mechanics and Engineering 2017; 36(4): 953-963.

[31] Wang SJ, Lu AZ, Tao JY, Zeng XT, Yin CL. Analytical solution for an arbitrary-shaped tunnel with full-slip contact lining in anisotropic rock mass. International Journal of Rock Mechanics and Mining Sciences 2020; 128: 104276.

[32] Wan MSP, Standing JR, Potts DM, Burland JB. Measured short-term subsurface ground displacements from EPBM tunnelling in London Clay. Géotechnique 2017a; 67(9): 748-779.

[33] Wan MSP, Standing JR, Potts DM, Burland JB. Measured short-term ground surface response to EPBM tunnelling in London Clay. Géotechnique 2017b; 67(5): 420-445.

[34] Wang HN, Chen XP, Jiang MJ, Song F, Wu L. The analytical predictions on displacement and stress around shallow tunnels subjected to surcharge loadings. Tunnelling and Underground Space Technology 2018; 71: 403-427.

[35] Yang XL, Wang JM. Ground movement prediction for tunnels using simplified procedure. Tunnelling and Underground. Space Technology 2011; 26: 462-471.

[36] Yi X, Kerryrowe R, Lee KM. Observed and calculated pore pressures and deformations induced by an earth balance shield. Canadian Geotechnical Journal 1993; 30:476-490.

[37] Yu HT, Cai C, Bobet A, Zhao X, Yuan Y. Analytical solution for longitudinal bending stiffness of shield tunnels. Tunnelling and Underground Space Technology 2019; 83: 27-34.

[38] Zeng B, Huang D. Soil deformation induced by Double-O-Tube shield tunneling with rolling based on stochastic medium theory. Tunnelling and Underground Space Technology 2016; 60: 165-177.

[39] Zhang ZG, Pan YT, Zhang MX, Lv XL, Jiang KM, Lia SN. Complex variable analytical prediction for ground deformation and lining responses due to shield tunneling considering groundwater level variation in clays. Computers and Geotechnics 2020; 120(4): 103443.

[40] Zhao Y. In situ soil testing for foundation performance prediction. PhD thesis, Cambridge University; 2008.

[41] Zheng G, Dai X, Diao Y, Zeng CF. Experimental and simplified model study of the development of ground settlement under hazards induced by loss of groundwater and sand. Natural Hazards 2016; 82(3):1869-1893.

[42] Zhou B. Tunnelling-induced ground displacements in sand. PhD thesis, University of Nottingham; 2015.

[43] Zhou M, Wang F, Du YJ, Liu MD. Laboratory evaluation of buried high-density polyethylene pipes subjected to localized ground subsidence. Acta Geotechnica 2019; 14(4):1081-1099.

[44] Zymnis DM, Chatzigiannellis Y, Whittle AJ. Effect of anisotropy in ground movements caused by tunneling. Géotechnique 2013; 63(13):1083-1102.